Cell Metabolism, Volume *24*

Supplemental Information

Long-Term Administration of Nicotinamide Mononucleotide Mitigates Age-Associated Physiological Decline in Mice

Kathryn F. Mills, Shohei Yoshida, Liana R. Stein, Alessia Grozio, Shunsuke Kubota, Yo Sasaki, Philip Redpath, Marie E. Migaud, Rajendra S. Apte, Koji Uchida, Jun Yoshino, and Shin-ichiro Imai

Supplemental Information

Long-term administration of nicotinamide mononucleotide mitigates age-associated physiological decline in mice

Kathryn F. Mills[1], Shohei Yoshida[2], Liana R. Stein[1,§], Alessia Grozio[1], Shunsuke Kubota[3], Yo Sasaki[4], Philip Redpath[5], Marie E. Migaud[5], Rajendra S. Apte[1,3], Koji Uchida[2], Jun Yoshino[6,*], and Shin-ichiro Imai[1,*]

[1]Department of Developmental Biology,
Washington University School of Medicine, St. Louis, MO 63110, USA
[2]Oriental Yeast Co., Tokyo, Japan
[3]Department of Ophthalmology,
[4]Department of Genetics,
Washington University School of Medicine, St. Louis, MO 63110, USA
[5]School of Pharmacy, Queen's University Belfast, UK
[6]Center for Human Nutrition, Division of Geriatrics and Nutritional Science, Department of Medicine,
Washington University School of Medicine, St. Louis, MO 63110, USA

*Co-corresponding authors
Shin-ichiro Imai, M.D., Ph.D. (Lead Contact)
Professor
Department of Developmental Biology
Department of Medicine (Joint)
Washington University School of Medicine
Campus Box 8103, 660 South Euclid Avenue,
St. Louis, MO 63110, USA
Tel: 314-362-7228 Fax: 314-362-7058 E-mail: imaishin@wustl.edu

Jun Yoshino, M.D., Ph.D.
Assistant Professor
Center for Human Nutrition
Division of Geriatrics and Nutritional Science, Department of Medicine
Campus Box 8031, 660 South Euclid Avenue,
St. Louis, MO 63110, USA
Tel: 314-362-8119 Fax: 314-362-8230 E-mail: jyoshino@dom.wustl.edu

§Present address: Gladstone Institute of Neurological Disease and Department of Neurology, University of California, San Francisco, CA 94158, USA.

A

Time	NMN100	NMN300
Week-17	91%	114%
Week-19	93%	97%
Week-23	92%	96%
Week-30	90%	96%
Week-31	91%	88%
Week-35	101%	103%

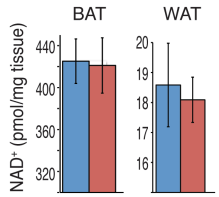

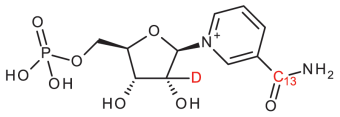

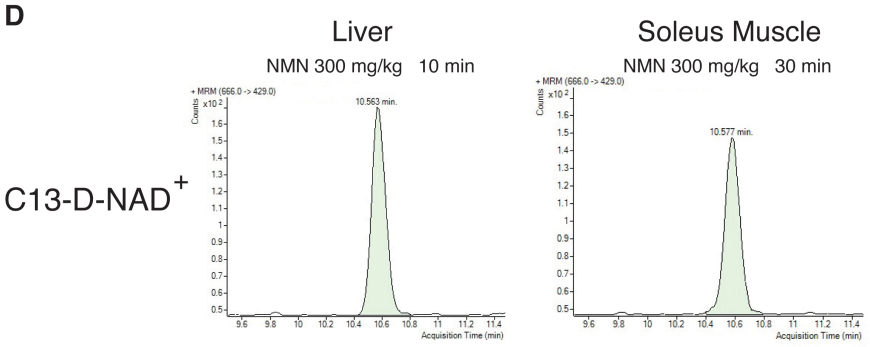

E

Purpose	Mice per group Control	NMN100	NMN300	Analysis
Monitoring	15	15	15	Body Temperature (monthly) Body Weight (weekly) Food/water intake (weekly) Fed blood collection- glucose, insulin, lipids (monthly) White blood cell counts (every three months)
Oxygen consumption	30	20	20	Oxygen consumption (6 and 12 month time points) Body composition Bone density Blood chemistries Eye examination
Physical activity	15	15	15	Multiple physical activity paramaters (12 month time point)
IPGTT & ITT	20	20	20	IPGTT and ITT (every three months) Fasted blood collection- insulin, lipids
Tissue collection	20	20	20	Tissue collection (5 every three months) NAD+ measurements Microarrays

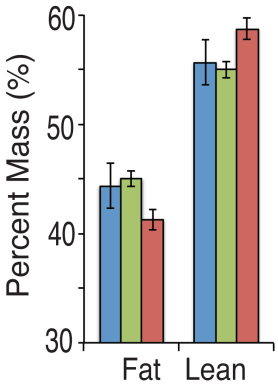

Figure S1; *Related to Figures 1 and 2*: NMN stability, NMN utilization for NAD⁺ biosynthesis, the number of mice for each analysis, and fat and lean mass of control and NMN-treated mice.

(A) NMN concentrations in freshly prepared NMN-containing drinking water and the leftover of used NMN-containing drinking water were periodically measured by HPLC throughout the entire period of NMN treatment. Percentages of NMN concentrations after 7-10 days in both 100 and 300 mg/kg/day groups were calculated (Relative to freshly prepared drinking water: NMN100 group; 93 ± 2%, NMN300 group; 99 ± 4%). (B) Three to four-month-old C57BL/6N mice were given NMN by oral gavage (300 mg/kg), and NAD^+ levels were evaluated after 1 hr in WAT and BAT by HPLC (control bars in blue; NMN 300 mg/kg bars in red; n=10 mice per group). All results presented as mean ± SEM. (C) The structure of doubly-labeled isotopic [^{13}C7, D2']-NMN (C13-D-NMN). (D)Mass spectrometric detection of doubly-labeled isotopic NAD^+ (C13-D-NAD^+) in the liver and soleus muscle at 10 and 30 min, respectively, after orally administering a 1:1 mixture of regular NMN and doubly-labeled isotopic NMN (C13-D-NMN). (E) The numbers of mice used for each analysis in this study. The mice for monitoring, oxygen consumption measurements, and physical activity measurements were used to monitor survival. (F) Body composition was determined by echo-MRI at 12 months of NMN treatment. Percent fat and lean masses were calculated for control (blue) and 100 (green) and 300 (red) mg/kg/day NMN-administered mice (n=5 for each group).

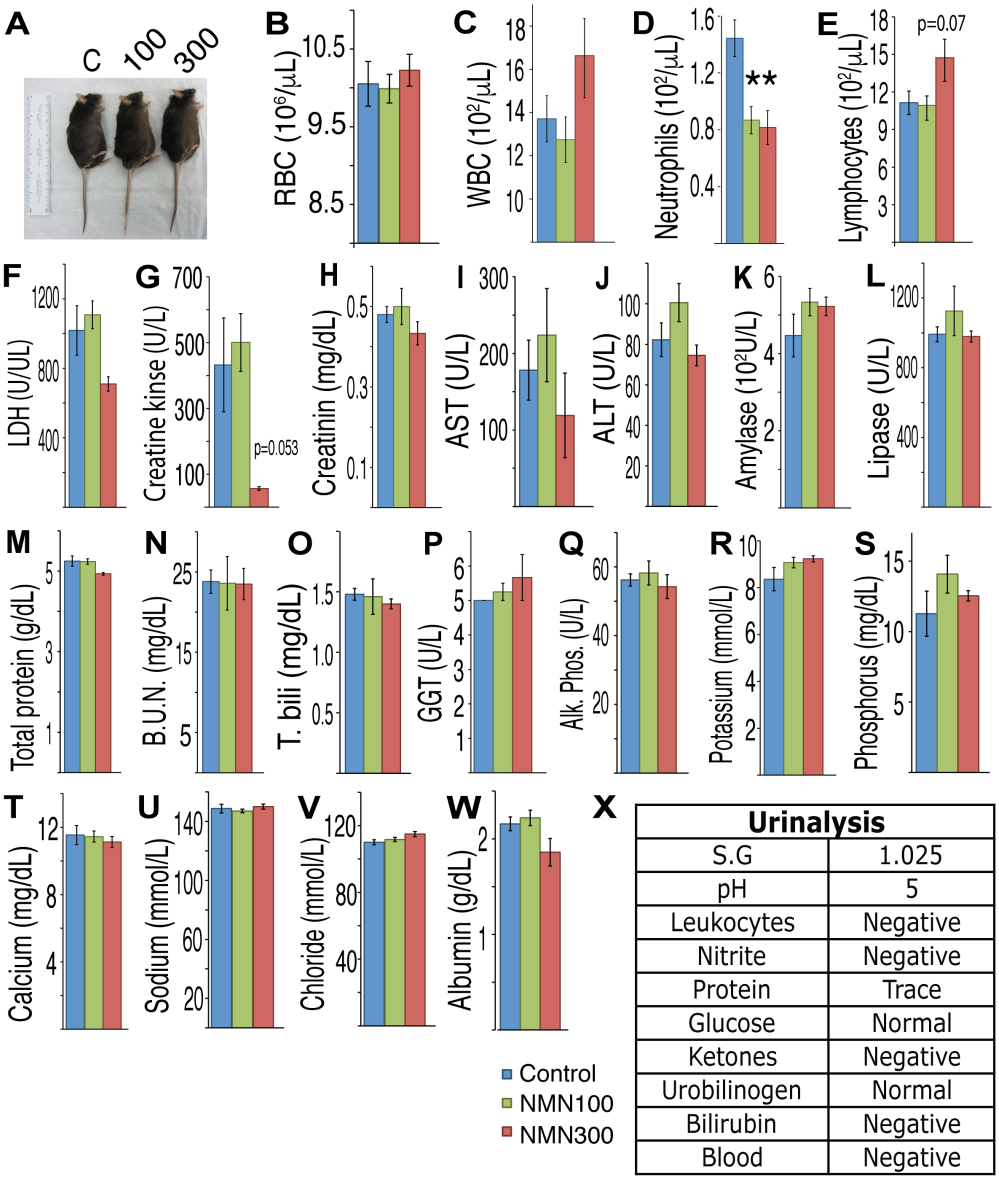

Urinalysis	
S.G	1.025
pH	5
Leukocytes	Negative
Nitrite	Negative
Protein	Trace
Glucose	Normal
Ketones	Negative
Urobilinogen	Normal
Bilirubin	Negative
Blood	Negative

Figure S2; *Related to Figure 2*: NMN displays no adverse effects throughout the entire intervention period.

Throughout the figure, controls are shown in blue, NMN 100 mg/kg/day in green, and NMN 300 mg/kg/day in red.

(A) Representative body lengths of mice from each group.

(B-E) After 12 months of their respective NMN doses, counts of red and white blood cells, neutrophils and lymphocytes were evaluated from whole blood samples in mice after an overnight fast (n=11-15 per group). Asterisks indicate a statistical significance versus control using one-way ANOVA (*p<0.05).

(F-W) Blood chemistries were analyzed 10-11 months after NMN administration. LDH (Lactate Dehydrogenase); AST (Aspartate Aminotransferase); ALT (Alanine Aminotransferase); B.U.N. (Blood Urea Nitrogen); T. bili (total bilirubin); GGT (Gamma-Glutamyl Transpeptidase); Alk. Phos (Alkaline Phosphatase) (n=5-7 per group).

(X) Test strips were used to measure specific gravity, pH, leukocytes, nitrites, protein, glucose, ketones, urobilinogen, bilirubin, and blood levels in the urine of mice. Table indicates representative results from mice in each group (n=10-12 per group). All results presented as mean ± SEM.

A

Cause of Death	Control	NMN100	NMN300
Thromboembolism/ atrial thrombososis or myocardial infarction	1 (424)		3 (197, 383, 419)
urinary tract obstruction or obstructive uropathy	1 (494)	2 (391, 447)	1 (427)
islet cell carcinoma	1 (495)		
post mortem degeneration too severe	1 (496)	1 (2)	2 (365, 452)
	(survival days shown in parentheses)		
	4 out of 60	3 out of 50	6 out of 50
% death	6.7%	6.0%	12.0%

B

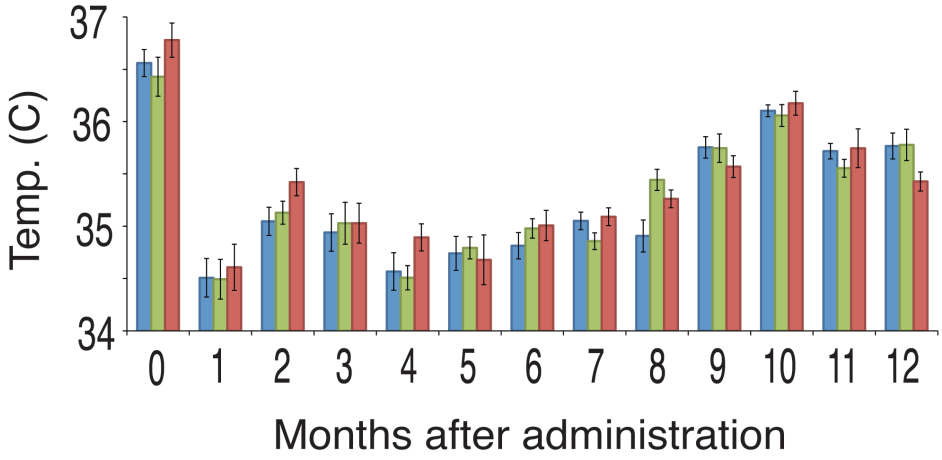

Figure S3; *Related to Figures 2 and 3*: The causes of death and rectal body temperature in control and 100 and 300 mg/kg/day NMN-administered groups throughout the entire 12-month intervention period.
(A) The causes of death and the numbers of each incidence in the survival-monitoring cohorts (see Figure S1D) throughout the entire 12-month intervention period. The causes of death were determined by necropsy.
(B) Rectal body temperature was measured monthly throughout the NMN treatment (n=14-15 mice per group). The data were collected in the afternoon at the beginning of the study (0 month). All other data were collected in the morning throughout the NMN treatment. All results presented as mean ± SEM.

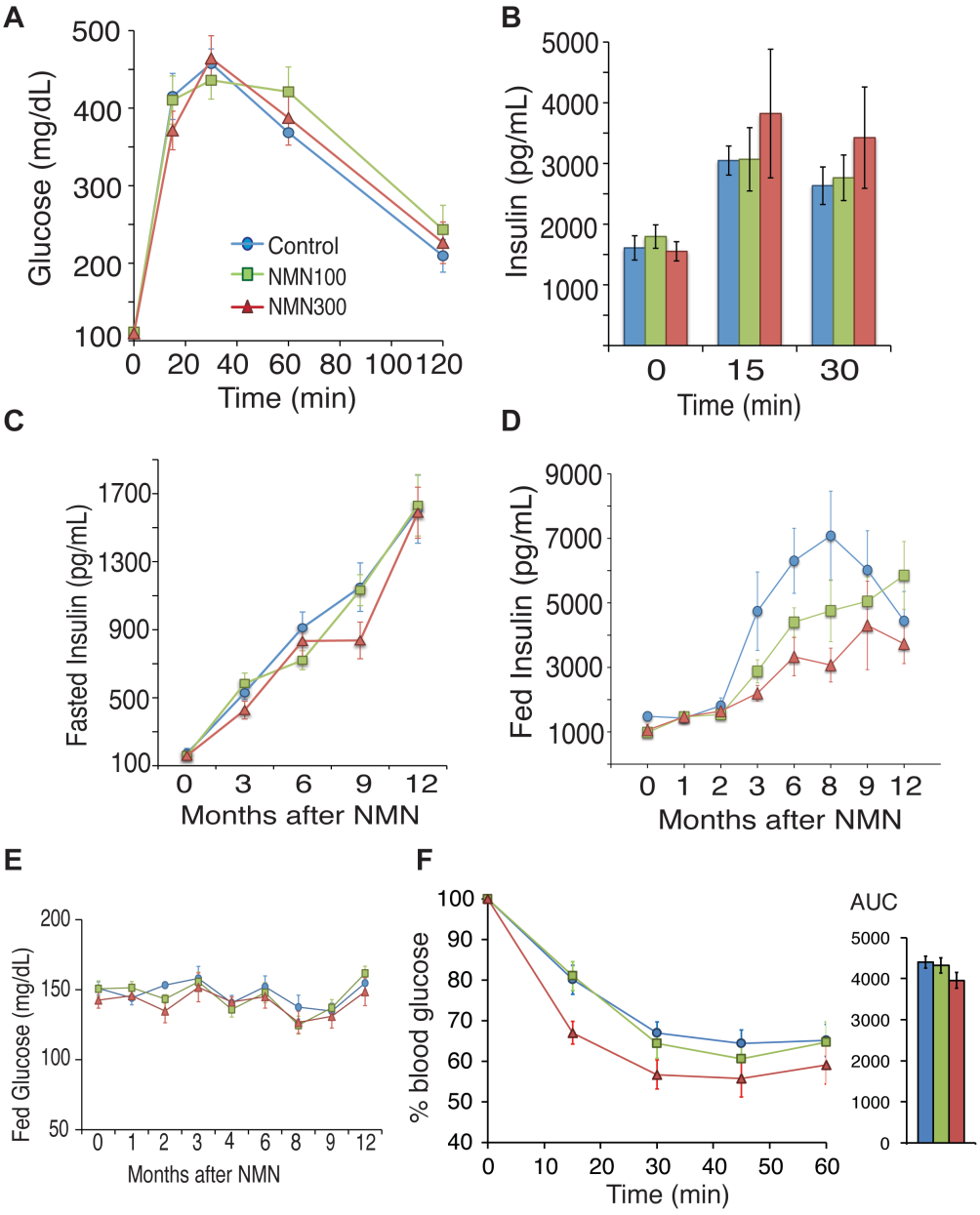

Figure S4; *Related to Figure 4*: NMN-treated mice display no differences in glucose tolerance or fed blood glucose levels, but show lower tendencies in fed and fasted insulin levels.
Throughout the figure, controls are shown in blue, NMN 100 mg/kg/day in green, and NMN 300 mg/kg/day in red.
(A) Intraperitoneal glucose tolerance test (IPGTT) after 12 months of NMN administration. Data shown here are the same individuals as those in Figure 4A (n=10-15 per group).
(B) Insulin levels were measured in plasma samples from the IPGTT (A) (n=10-15 per group).
(C) Fasted plasma insulin levels were analyzed every three months from mice, after an overnight fast (n=10-15 per group).
(D) Fed plasma insulin levels were analyzed monthly (n=9-15).
(E) Blood glucose levels were measured monthly from fed mice (n= 9-15).

A

Skeletal muscle

PROBE_ID	Symbol	Z ratio (12M/6M) control	NMN	Z difference
ILMN_2597660	*Pcdh1*	-2.55	0.70	3.24
ILMN_1212949	*Ncstn*	2.37	-0.75	3.12
ILMN_1258028	*Gal3st1*	-2.48	0.57	3.05
ILMN_1245509	*B3galt5*	3.39	0.41	2.98
ILMN_2806549	*Prm1*	-2.78	0.19	2.97
ILMN_2853360	*Pex13*	-3.46	-0.82	2.65
ILMN_2717037	*Adcyap1r1*	2.68	0.06	2.62
ILMN_1257051	*Glt25d2*	-3.21	-0.60	2.61
ILMN_1212612	*Rcan2*	-2.61	-0.18	2.42
ILMN_1239557	*Ugt8a*	-3.11	-0.72	2.40
ILMN_2466926	*Zfp235*	-3.49	-1.10	2.39
ILMN_2598402	*Parp8*	-3.92	-1.60	2.32
ILMN_1212835	*Ugt1a6a*	2.81	0.51	2.31
ILMN_3160568	*Ankrd50*	-3.00	-0.70	2.30
ILMN_3143604	*Gng2*	-3.23	-0.94	2.29
ILMN_1235612	*Lenep*	-2.63	-0.40	2.24
ILMN_2750219	*BC066135*	3.17	0.95	2.22
ILMN_2938507	*Casz1*	-2.62	-0.42	2.20
ILMN_3160416	*2900024O10Rik*	-3.03	-0.87	2.16
ILMN_3041584	*Cuta*	2.04	-0.11	2.15

WAT

PROBE_ID	Symbol	Z ratio (12M/6M) control	NMN	Z difference
ILMN_1243812	*Plekha3*	-4.01	0.80	4.81
ILMN_2658144	*Palm*	-3.02	1.43	4.45
ILMN_2696163	*2010110P09Rik*	-3.29	1.02	4.31
ILMN_1229977	*Cux1*	-3.29	0.46	3.76
ILMN_1217939	*B230120H23Rik*	-3.06	0.61	3.67
ILMN_1243095	*Vbp1*	-3.64	-0.08	3.55
ILMN_2882189	*Tmprss11b*	-3.05	0.21	3.26
ILMN_2477870	*Vit*	-3.13	0.07	3.20
ILMN_2714252	*Kcnj3*	-3.20	-0.05	3.15
ILMN_2614990	*Akap3*	-2.93	0.22	3.15
ILMN_2614759	*Timp3*	-3.63	-0.48	3.15
ILMN_2974737	*BC065085*	3.04	-0.06	3.10
ILMN_2745602	*Olfr996*	3.35	0.32	3.04
ILMN_1216803	*Idi2*	-2.82	0.21	3.02
ILMN_2629755	*Hook1*	2.46	-0.53	3.00
ILMN_1251206	*Yme1l1*	-3.67	-0.69	2.97
ILMN_1253150	*Otud6b*	-3.66	-0.69	2.97
ILMN_1213817	*Mup3*	-2.52	0.43	2.94
ILMN_2841917	*LOC622665*	-3.92	-0.98	2.94
ILMN_2748755	*Heph*	-3.58	-0.64	2.94

Liver

PROBE_ID	Symbol	Z ratio (12M/6M) control	NMN	Z difference
ILMN_3008068	*Scara5*	-2.55	1.28	3.83
ILMN_2664937	*Rnf138*	-2.40	0.34	2.74
ILMN_2650915	*Jmjd2b*	-3.22	-0.70	2.51
ILMN_2724371	*Phldb1*	-2.52	-0.04	2.48
ILMN_2628875	*Jph2*	3.20	0.90	2.30
ILMN_2695360	*Lcn13*	-3.56	-1.30	2.26
ILMN_2716389	*Smpd3*	-2.93	-0.70	2.23
ILMN_2620037	*Tmco6*	2.69	0.64	2.05
ILMN_1236610	*Socs6*	-3.08	-1.10	1.98
ILMN_2652857	*Ifi47*	-4.34	-2.37	1.97
ILMN_2650049	*Sts*	-2.94	-1.00	1.94
ILMN_2634728	*Bbs9*	-2.92	-1.04	1.88
ILMN_1227900	*Il12rb1*	-2.53	-0.68	1.85
ILMN_2466121	*Twistnb*	-4.07	-2.29	1.78
ILMN_1255033	*LOC100047082*	2.44	0.67	1.77
ILMN_2648189	*Klf10*	-2.81	-1.06	1.75
ILMN_2708190	*Angptl3*	-3.52	-1.78	1.75
ILMN_2610678	*Rgs3*	2.80	1.08	1.72
ILMN_1214057	*Psmd11*	-2.45	-0.73	1.72
ILMN_1258035	*Gpc4*	-3.29	-1.59	1.70

B

Skeletal muscle

Geneset name	Z score (12M/6M) control	NMN	Z difference
CELLULAR_COMPONENT_ASSEMBLY	-3.86	0.34	4.20
MACROMOLECULAR_COMPLEX_ASSEMBLY	-3.76	0.26	4.01
PROTEIN_COMPLEX_ASSEMBLY	-3.98	-0.32	3.66
NEUROPEPTIDE_BINDING	2.35	-0.87	3.22
NEUROPEPTIDE_RECEPTOR_ACTIVITY	2.35	-0.87	3.22
REGULATION_OF_RHO_GTPASE_ACTIVITY	-3.61	-0.44	3.17
PHOSPHORYLATION	-4.42	-1.27	3.16
REGULATION_OF_GTPASE_ACTIVITY	-3.56	-0.55	3.01
ATPASE_ACTIVITY	-4.72	-1.75	2.97
REGULATION_OF_RHO_PROTEIN_SIGNAL_TRANSDUCTION	-3.41	-0.44	2.97
CYTOPLASMIC_PART	-4.65	-1.72	2.93
PROTEIN_AMINO_ACID_PHOSPHORYLATION	-4.59	-1.71	2.89
MOLECULAR_ADAPTOR_ACTIVITY	-2.00	0.83	2.83
DNA_PACKAGING	-2.35	0.47	2.82
ADENYL_NUCLEOTIDE_BINDING	-2.70	0.03	2.73
MAGNESIUM_ION_BINDING	-1.97	0.75	2.72
ATPASE_ACTIVITY_COUPLED	-4.19	-1.48	2.71
NUCLEOSIDE_TRIPHOSPHATASE_ACTIVITY	-4.59	-1.88	2.71
REGULATION_OF_RAS_GTPASE_ACTIVITY	-3.92	-1.22	2.70
FOCAL_ADHESION_FORMATION	-2.90	-0.22	2.68

WAT

Geneset name	Z score (12M/6M) control	NMN	Z difference
CYTOKINE_ACTIVITY	3.05	-0.63	3.69
LEUKOCYTE_ACTIVATION	4.47	0.99	3.48
CELL_ACTIVATION	4.71	1.45	3.26
NEUROPEPTIDE_BINDING	3.35	0.13	3.22
NEUROPEPTIDE_RECEPTOR_ACTIVITY	3.35	0.13	3.22
LYMPHOCYTE_ACTIVATION	4.27	1.05	3.22
IMMUNE_RESPONSE	1.98	-1.21	3.19
IMMUNE_SYSTEM_PROCESS	1.97	-1.15	3.11
CELL_MATRIX_ADHESION	-2.93	-0.05	2.88
REGULATION_OF_MYELOID_CELL_DIFFERENTIATION	-3.99	-1.15	2.84
CELL_SUBSTRATE_ADHESION	-2.70	0.10	2.80
CYTOPLASMIC_PART	-4.32	-1.58	2.74
CHANNEL_REGULATOR_ACTIVITY	2.37	-0.22	2.59
POSITIVE_REGULATION_OF_LYMPHOCYTE_ACTIVATION	3.66	1.09	2.57
CYTOKINE_PRODUCTION	2.42	-0.11	2.53
NEGATIVE_REGULATION_OF_CELL_DIFFERENTIATION	-2.62	-0.12	2.51
BEHAVIOR	1.99	-0.46	2.44
REGULATION_OF_CELL_DIFFERENTIATION	-2.19	0.24	2.43
TRANSMEMBRANE_RECEPTOR_PROTEIN_SERINE_THREONINE_KINASE_SIGNALING_PATHWAY	-2.11	0.31	2.42
NUCLEOTIDYLTRANSFERASE_ACTIVITY	-3.73	-1.34	2.40

Liver

Geneset name	Z score (12M/6M) control	NMN	Z difference
EXOCYTOSIS	-2.15	0.83	2.98
PHOSPHORUS_OXYGEN_LYASE_ACTIVITY	-3.03	-0.75	2.28
SYNAPTIC_VESICLE	2.69	0.50	2.19
REPRODUCTION	2.31	0.33	1.98
CYCLASE_ACTIVITY	-2.91	-0.95	1.96
REPRODUCTIVE_PROCESS	1.96	0.19	1.77
PHAGOCYTOSIS	-2.85	-1.10	1.76
ENDOPLASMIC_RETICULUM_MEMBRANE	-2.26	-0.53	1.73
POSITIVE_REGULATION_OF_DEVELOPMENTAL_PROCESS	-2.64	-0.92	1.72
POSITIVE_REGULATION_OF_TRANSLATION	-1.99	-0.29	1.71
G1_S_TRANSITION_OF_MITOTIC_CELL_CYCLE	-2.76	-1.07	1.69
VESICLE_MEDIATED_TRANSPORT	-2.94	-1.30	1.64
INTERLEUKIN_2_PRODUCTION	-2.65	-1.01	1.63
POSITIVE_REGULATION_OF_SECRETION	2.00	0.43	1.56
HEMATOPOIETIN_INTERFERON_CLASSD200_DOMAIN_CYTOKINE_RECEPTOR_BINDING	2.14	0.61	1.53
NUCLEAR_ENVELOPE_ENDOPLASMIC_RETICULUM_NETWORK	-2.12	-0.60	1.53
RESPONSE_TO_IONIZING_RADIATION	-2.21	-0.79	1.42
METAL_ION_TRANSPORT	2.92	1.52	1.40
INDUCTION_OF_APOPTOSIS_BY_INTRACELLULAR_SIGNALS	-2.37	-0.99	1.38
POTASSIUM_ION_TRANSPORT	2.85	1.48	1.37

(F) Insulin tolerance tests were performed for all (not body weight-matched) mice in each cohort. Relative blood glucose levels were calculated (n=18-23 per group). Glucose levels at each time point are normalized to that at 0 min. AUCs are also shown at right.
All results presented as mean ± SEM.

Figure S5; *Related to Figure 5*: Long-term NMN administration prevents age-associated changes in gene expression profiles and biological pathways in peripheral tissues.

Microarray analysis was conducted to compare gene expression profiles of skeletal muscle, white adipose tissue (WAT), and liver in control and NMN 300 mg/kg/day mice after 6 and 12 months of NMN administration (n=4 per group). (A) Genes that were significantly changed in control mice were selected by the rank product method (false discovery ratios [FDR] < 0.05) and 20 top genes are listed following the sum of the absolute values of Z ratios between two comparisons (Z difference). (B) Biological pathways that were significantly changed in control mice were selected by the parametric analysis of gene-set enrichment (PAGE) analysis (P <

0.05) and 20 top pathways are listed following the sum of the absolute values of Z scores between two comparisons (Z difference).

Supplemental Experimental Procedures

Isotopic tracing experiment

Doubly-labeled [^{13}C7, D2']-NMN (C13-D-NMN) was synthesized from doubly-labelled [^{13}C7, D2']-nicotinamide riboside (NR) according to the procedure described previously (Lee et al., 1999). Three month-old male mice were orally administered with a 1:1 mixture of regular NMN and doubly-labeled C13-D-NMN at a total dose of 300mg/kg or PBS after an overnight fast. Liver and soleus muscle were collected at 10 and 30 min time points after oral gavage. A 1:1 mixture of reagent-grade methanol and water (4°C) were added to the frozen tissue (60-100 μL/mg tissue). After sonication, extracts were centrifuged at 12,000 x g for 10 min at 4°C. Chloroform was added to the extracts at a ratio of 1:1 (v/v), thoroughly shaken for 30 s, and centrifuged at 12,000 x g for 10 min at 4°C. The upper phase (methanol and water) was separated from the lower (organic) phase and extracted with chloroform for three times. The methanol/water fraction was then lyophilized by speed vacuum at room temperature, reconstituted with 5mM ammonium formate (20 mg/mL), and centrifuged at 12,000 x g for 10 min. Cleared supernatants (10 μL) were used for analysis. Serial dilutions of NAD^+ at concentrations ranging 62.5 - 2000 nmol/L in 5 mM ammonium formate were used for calibration. Liquid chromatography was performed by HPLC (1290; Agilent) with Atlantis T3 (LC 2.1 x 150mm, 3 mm; Waters) at a flow rate of 0.15 ml/min with 5 mM ammonium formate for mobile phase A and 100% methanol for mobile phase B. Metabolites were eluted with gradients of 0-10 min, 0–70% B; 10-15 min, 70% B; 16–20 min, 0% B (Hikosaka et al., 2014). The metabolites were analyzed with a Triple Quadrupole mass spectrometer (6460 MassHunter; Agilent) under positive ESI multiple reaction monitoring (MRM) using parameters for NAD^+ (664>428) and C13-D-NAD^+ (666>429). Fragmentation, collision, and post acceleration voltages were 160, 22, and 7, respectively. NAD^+ or C13-D-NAD^+ peaks were identified using the MassHunter quantitative analysis tool (Agilent). Areas under the curves of C13-D-NAD^+ were calculated by subtracting the background values of PBS controls.

Indirect calorimetry measurements

Mice were individually housed in the chamber with a 12-h light/12-h dark cycle in ambient temperature of 22-24°C and allowed a minimum of 12 hours to acclimate to the chamber before data collection. VO_2 and VCO_2

rates were determined under Oxymax system settings as follows: air flow, 0.6 l/min; sample flow, 0.5 l/min; settling time, 6 min; and measuring time, 3 min. The system was calibrated against a standard gas mixture to measure O_2 consumed (VO_2, ml/kg/hr) and CO_2 generated (VCO_2, ml/kg/hr). Oxygen consumption (VO_2) and respiratory quotient (ratio of VCO_2/VO_2) were evaluated over a 24-h period. Energy expenditure (EE) was calculated as the product of the calorific value of oxygen (3.815 + 1.232 x respiratory quotient) and the volume of O_2 consumed.

Microarrays

The background-subtracted raw microarray data were subjected to the quantile normalization and false discovery rates (FDR) were calculated using the Rank Products Analysis (Breitling et al., 2004). FDR < 0.05 was considered significantly changed. The background-subtracted raw microarray data were also normalized by Z score transformation to obtain Z ratios. We applied the Parametric Analysis of Gene Set Enrichment (PAGE) to identify biological pathways significantly changed by aging process as previously described (Kim and Volsky, 2005; Yoshino et al., 2011). In brief, gene sets were obtained from http://www.broad.mit.edu/gsea/ (GO gene sets, C5 collection) and Z scores and P values were calculated for each gene set. P value < 0.05 was considered significantly changed. All data were analyzed by the R statistical software package (available at http://www.bioconductor.org). The background-substracted normalized data were also used for principal component analysis (PCA).

High-resolution respirometry

Fresh soleus muscle was prepared as previously described (Kuznetsov et al., 2008). Briefly, isolations were performed in a cold room at 4°C or on ice. The soleus muscle (~25mg) was immediately removed from mice with minimal separation of the fibers and placed in ice-cold BIOPS buffer (50 mM K-MES, 20 mM taurine, 0.5 mM DTT, 6.56 mM $MgCl_2$, 5.77 mM ATP, 15 mM phosphocreatine, 20 mM imidazole; [pH 7.1], adjusted with 5 N KOH at 0°C, and added 10 mM Ca-EGTA buffer [2.77 mM CaK_2EGTA + 7.23mM K_2EDTA; 0.1 μM free calcium]). The muscle was trimmed of connective tissue and fat under a dissection microscope and cut into small segments (1-4 mg). The tissues were then treated with freshly prepared 15 μg/mL saponin and incubated in a cold room for 20 minutes. Following permeabilization, samples were transferred to Mir05 buffer (110 mM sucrose, 60mM potassium lactobionate, 20mM taurine, 20mM HEPES, 10mM KH_2PO_4, 3 mM $MgCl_2$•6 H_2O, 0.5mM EGTA, 1g/liter BSA (fraction V), [pH 7.1]) for 10 minutes. Samples were transferred again to Mir05 buffer until analysis. Wet weight measurements were made after incubation, and two 2-ml Oroboros chambers, kept at 37ºC, were loaded with 1-5 mg of permeabilized soleus muscle in MiRO5 respiration medium plus 25 μM blebbistatin and 20 mM creatine (Perry et al., 2011). 0.5 mM malate was added as an oxidative substrate

followed by 10mM glutamate and 5mM pyruvate to assess stage 2 (LEAK) respiration. 5mM ADP was then added to stimulate respiration of complex I, following with 10mM succinate to interrogate complex II. 10μM cytochrome c was added to confirm the integrity of mitochondrial membranes, with the samples demonstrating an average of <13% increase in respiration. Titrating steps of 0.5 μM FCCP were added to assess maximal respiratory capacity. The assay was completed by addition of 1μM rotenone to inhibit complex I.

Western blotting of mitochondrial extracts

Mitochondrial extracts were prepared from fresh soleus muscle as previously described (Dimauro et al., 2012). SDS-PAGE was performed on a 12% Tric-HCl gel (Bio-Rad). Samples containing 9 μg of protein were not boiled, due to manufacturer's instructions of the primary antibody, before loading with 5x Laemmli buffer. The proteins were transferred to a PVDF membrane (Millipore), and the membrane was blocked with 5% nonfat milk. The membrane was probed with a primary total OXPHOS rodent antibody cocktail (Abcam; ab110413), and the same blot was re-probed with anti-VDAC1 (B-6) antibody (Santa Cruz Biotechnology; sc-390996). Signals were visualized using the ECL regular and ECL advance detection systems (GE Healthcare) and quantified using Adobe Photoshop.

Analysis of photoreceptor function and tear production

Bilateral flash electroretinography (ERG) measurements were performed using a UTAS-E3000 Visual Electrodiagnostic System running EM for Windows (LKC Technologies, Inc., Gaithersburg MD). Mice were dark-adapted overnight, then anesthetized with 86.9 mg/kg ketamine and 13.4 mg/kg xylazine under dim red illumination for electrode placement and testing. Body temperature was maintained at 37.5 ± 1.0°C with a heating pad controlled by a rectal temperature probe (FHC Inc., Bowdoin ME). The mouse head was positioned just inside the opening of the Ganzfeld dome, and pupils were dilated with 1.0% atropine sulfate (Bausch & Lomb, Tampa FL). The recording electrode was a platinum loop 2.0 mm in diameter, positioned in a drop of 1.25% hydroxypropyl methylcellulose (GONAK; Akorn Inc., Buffalo Grove IL) on the corneal surface of each eye. The reference needle electrode was inserted under the skin at the vertex of the skull. The ground electrode was inserted under the skin of the mouse's back or tail. The stimulus (trial) consisted of a brief, full-field flash (10 ms) either in darkness, or in the presence of dim (30.0 cd/m^2) background illumination after 10 minutes adaptation time to the background light. The initiation of the flash was taken as time zero. The response was recorded over 250 ms plus 25 ms of pre-trial baseline. Responses from several trials were averaged. The amplitude of the a-wave was measured from the average pre-trial baseline to the most negative point of the average trace, and the b-wave amplitude from that point to the highest positive point, without subtracting oscillatory potentials. The log light intensity (log [$cd*s/m^2$]) was calculated based on the manufacturer's

calibrations. The amplitudes (in microvolts) of dark-adapted a- and b-waves and light-adapted b-waves were measured from the lowest point of the raw averaged response trace (occurring prior to 50 ms after the flash) to the subsequent highest point.

For the measurement of tear production, a phenol red-impregnated thread is placed on the temporal side of the lower eyelid margin for 30 seconds without anesthesia. Then, the length of the moistened fragment is measured. Tear production from both left and right eyes of each mouse was measured.

Supplemental references

Breitling, R., Armengaud, P., Amtmann, A., and Herzyk, P. (2004). Rank products: a simple, yet powerful, new method to detect differentially regulated genes in replicated microarray experiments. FEBS Lett. 573, 83-92.

Dimauro, I., Pearson, T., Caporossi, D., and Jackson, M.J. (2012). A simple protocol for the subcellular fractionation of skeletal muscle cells and tissue. BMC Res. Notes 5, 513.

Hikosaka, K., Ikutani, M., Shito, M., Kazuma, K., Gulshan, M., Nagai, Y., Takatsu, K., Konno, K., Tobe, K., Kanno, H., et al. (2014). Deficiency of nicotinamide mononucleotide adenylyltransferase 3 (nmnat3) causes hemolytic anemia by altering the glycolytic flow in mature erythrocytes. J. Biol. Chem. 289, 14796-14811.

Kim, S.Y., and Volsky, D.J. (2005). PAGE: parametric analysis of gene set enrichment. BMC Bioinformatics 6, 144.

Kuznetsov, A.V., Veksler, V., Gellerich, F.N., Saks, V., Margreiter, R., and Kunz, W.S. (2008). Analysis of mitochondrial function in situ in permeabilized muscle fibers, tissues and cells. Nat. Protoc. 3, 965-976.

Lee, J., Churchil, H., Choi, W.-B., Lynch, J.E., Roberts, F.E., Volante, R.P., and Reider, P.J. (1999). A chemical synthesis of nicotinamide adenine dinucleotide. Chem. Commun. 8, 729-730.

Perry, C.G., Kane, D.A., Lin, C.T., Kozy, R., Cathey, B.L., Lark, D.S., Kane, C.L., Brophy, P.M., Gavin, T.P., Anderson, E.J., et al. (2011). Inhibiting myosin-ATPase reveals a dynamic range of mitochondrial respiratory control in skeletal muscle. Biochem. J. 437, 215-222.

Yoshino, J., Mills, K.F., Yoon, M.J., and Imai, S. (2011). Nicotinamide mononucleotide, a key NAD(+) intermediate, treats the pathophysiology of diet- and age-induced diabetes in mice. Cell Metab. 14, 528-536.